

X-ray diffraction study and theoretical calculations on the X-phase, $\text{Al}_9(\text{Co}, \text{Ni})_4$

S. KATRYCH[†], M. MIHALKOVIC[‡], V. GRAMLICH[†],
M. WIDOM[§] and W. STEURER^{*†}

[†]Laboratory of Crystallography, Wolfgang-Pauli-Strasse 10,
ETH Zurich, 8093 Zurich, Switzerland

[‡]Institute of Physics, Slovak Academy of Sciences,
845 11 Bratislava, Slovakia

[§]Department of Physics, Carnegie Mellon University, Pittsburgh, USA

(Received 6 May 2005; in final form 5 July 2005)

The structure of the X-phase was solved based on single-crystal X-ray diffraction data. The previously unknown ternary compound in the system Al–Co–Ni is representative of a new structure type with Pearson symbol $mS26$, lattice parameters $a = 12.146(2) \text{ \AA}$, $b = 4.0702(5) \text{ \AA}$, $c = 7.652(1) \text{ \AA}$, $\beta = 105.88(1)^\circ$, $V = 363.83(9) \text{ \AA}^3$, and spacegroup $C2/m$. The stability of the monoclinic structure and the Co/Ni ordering was studied by first-principles total-energy calculations. The lowest-energy variant has composition $\text{Al}_{18}\text{Co}_5\text{Ni}_3$. There are indications that the X-phase is an entropy-stabilized high-temperature phase.

1. Introduction

The X-phase was first mentioned in literature in 1991 [1]. The author identified the stability fields of this compound on different isothermal sections. Based on Guinier film data, the orthorhombic lattice parameters $a = 17.68 \text{ \AA}$, $b = 11.66 \text{ \AA}$, $c = 12.27 \text{ \AA}$ were derived. Later on, the existence of the X-phase was confirmed [2–4], however, its structure has never been determined up to now. The X-phase is of special interest because it coexists with decagonal Al–Co–Ni in a broad concentration and temperature range. Therefore, the knowledge of its structure and stability may help promoting our understanding of the decagonal phase. The present work, based on experimental data as well as on theoretical calculations fills one of the last white spots in the ternary system Al–Co–Ni.

2. Experimental

Samples with compositions $\text{Al}_{69.8}\text{Co}_{19.2-x}\text{Ni}_{11+x}$, $x = 0, 1, 2$, all inside of the published stability field of the X-phase at 900°C [2], were prepared by arc melting compacts of the elements (Al 99.99%, Co 99.998%, Ni 99.998%). Afterwards, the

*Corresponding author. Email: walter.steurer@mat.ethz.ch

prealloys were heated to 1350°C in a high-vacuum resistance furnace (PVA MOV 64), held for 45 min at this temperature and cooled down within 18 hours to 850°C, 900°C, 960°C for $\text{Al}_{69.8}\text{Co}_{19.2}\text{Ni}_{11}$, $\text{Al}_{69.8}\text{Co}_{18.2}\text{Ni}_{12}$ and $\text{Al}_{69.8}\text{Co}_{17.2}\text{Ni}_{13}$, respectively. Subsequently, the samples were annealed for 60 hours at these final temperatures and quenched to ambient temperature by jetting cold argon into the sample chamber.

All samples were characterized by powder (STOE diffractometer, $\text{CuK}\alpha_1$) as well as by single-crystal X-ray diffraction (Xcalibur PX, Oxford diffraction, $\text{MoK}\alpha$). Data reduction and numerical absorption correction were performed using CRYSTALIS [5].

3. Results and discussion

The X-phase forms at 1002°C in a ternary peritectoidal reaction from $\beta + (\text{Co}, \text{Ni})_2\text{Al}_5 + \text{D}$, with β denoting the disordered B2 (i.e. CsCl-type) phase and D the decagonal phase [2]. According to the powder X-ray diffraction patterns (figure 1), only the samples $\text{Al}_{69.8}\text{Co}_{19.2}\text{Ni}_{11}$ and $\text{Al}_{69.8}\text{Co}_{18.2}\text{Ni}_{12}$ contain X-phase beside $\text{D} + \beta'$ and only β' , respectively. β' , $\text{Al}_4(\text{Co}, \text{Ni})_3$ is a $4 \times 4 \times 4$ superstructure of the β -phase. As before [1, 2], no single-phase samples could be obtained. However, several single crystals of sufficient size ($0.05 \times 0.05 \times 0.01 \text{ mm}^3$) and quality for X-ray diffraction formed in these multi-phase alloys during thermal treatment.

The crystal structure was solved by direct methods and refined using SHELXS-97 and SHELXL-97, respectively [6, 7]. We checked the space groups, Cm , $C2$ and $C2/m$. Since we found no significant difference in R-values, we assigned centrosymmetric space group $C2/m$ to this new phase. A final goodness-of-fit of 0.81 and R-factors of $R=0.177$, $wR=0.104$ for all 1838 unique reflections within $5^\circ \leq \theta \leq 48.5^\circ$ and $R=0.050$, $wR=0.092$ for the 664 reflections with $I > 2s(I)$

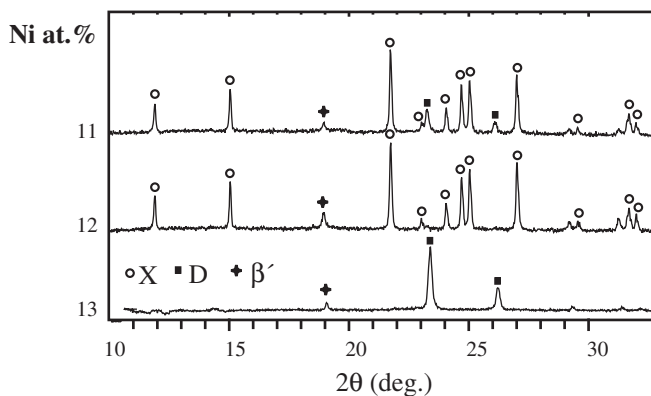


Figure 1. Powder X-ray diffraction patterns of the samples with nominal composition $\text{Al}_{69.8}\text{Co}_{19.2-x}\text{Ni}_{11+x}$, $x=0, 1$, and 2 . No variation can be seen in lattice parameters of the X-phase (marked by open circles) in the two samples with $x=0$ and 1 where it can be observed.

Table 1. Atomic coordinates, equivalent isotropic and anisotropic displacement parameters ($\text{\AA}^2 \times 10^3$) for $\text{Al}_9(\text{Co},\text{Ni})_4$. The anisotropic displacement factor reads: $\exp(-2\pi^2[h^2a^{*2}U_{11} + \dots + 2hka^*b^*U_{12}])$, $U(\text{eq}) = 1/3\Sigma_i\Sigma_jU_{ij}a_i^*a_j^*$.

Atom	X	y	z	$U(\text{eq})$	U_{11}	U_{22}	U_{33}	U_{23}	U_{13}	U_{12}
TM(1)	0.2934(1)	0	0.1272(1)	10(1)	10(1)	12(1)	8(1)	0	2(1)	0
TM(2)	0.3863(1)	1/2	-0.2909(1)	11(1)	12(1)	10(1)	10(1)	0	4(1)	0
Al(1)	0.1814(1)	1/2	-0.4551(1)	11(1)	10(1)	13(1)	10(1)	0	2(1)	0
Al(2)	0.5046	0	-0.2623(1)	12(1)	10(1)	11(1)	15(1)	0	2(1)	0
Al(3)	0.2981(1)	0	-0.1900(1)	12(1)	15(1)	11(1)	13(1)	0	6(1)	0
Al(4)	0.4032(1)	1/2	0.0542(1)	12(1)	10(1)	12(1)	13(1)	0	2(1)	0
Al(5)	1/2	1/2	1/2	20(1)	25(1)	20(1)	20(1)	0	12(1)	0

resulted (R is based on $|F|$ and wR on $|F|^2$). 41 parameters were refined with anisotropic atomic displacement parameters being restrained.

The atomic parameters are listed in table 1. All sites are fully occupied, the atomic displacement parameters are physically reasonable. The higher values for Al(5) may indicate preferred occurrence of vacancies at this site. The shortest distances are 2.3827(6) Å for Al–TM (transition metal) and 2.6375(9) Å for Al–Al. This compares to the sum of covalent radii of 2.41 Å for Al–Co (2.40 Å for Al–Ni) and is significantly larger than the sum of 2.50 Å for Al–Al.

The crystal structure is depicted in figure 2. It consists of two flat atomic layers perpendicular to the y -direction, related to each other by C centring. The layers can be seen as built from distorted pentagonal structure motifs (figure 3). Along the z -direction, the TM atoms form two columns of face sharing trigonal antiprisms, which can also be seen as distorted octahedra (edge lengths between 4.07 and 4.76 Å). The Al atoms are arranged in chains of alternating, one-corner sharing rhombohedra and octahedra interwoven with one of the two different TM columns. The other TM column contains centred hexagonal Al prisms.

If only those TM–TM distances (with 2.798 Å and 2.814 Å) are considered that are before the large gap (from 2.82 Å to 4.07 Å) in the distances histogram, then zigzag chains of TM atoms are obtained along the y -direction. Each one of these TM atoms is part of a dumbbell of two TM atoms.

The pentagonal structure motifs shown in figure 3 form distorted pentagonal prisms (edge lengths between 4.432 Å and 5.102 Å) running along the y -direction. The arrangement of these pentagonal prisms is very similar to that in metastable $m\text{-Al}_{11}\text{Co}_4$ and stable $o\text{-Al}_{13}\text{Co}_4$ (see fig. 5.2.1.1-1 of [8]). The packing of the layers, however, is different in all these cases.

4. Theoretical calculations

We performed first-principles total-energy calculations of Co/Ni order in the X-phase for the full range of $\text{Al}_9(\text{Co}, \text{Ni})_4$ compositions. Our calculations employed PAW potentials (an all-electron generalization of pseudopotentials) as implemented in the electronic density functional theory program VASP [9, 10]. The generalized gradient approximation (GGA) was used for exchange–correlation functional.

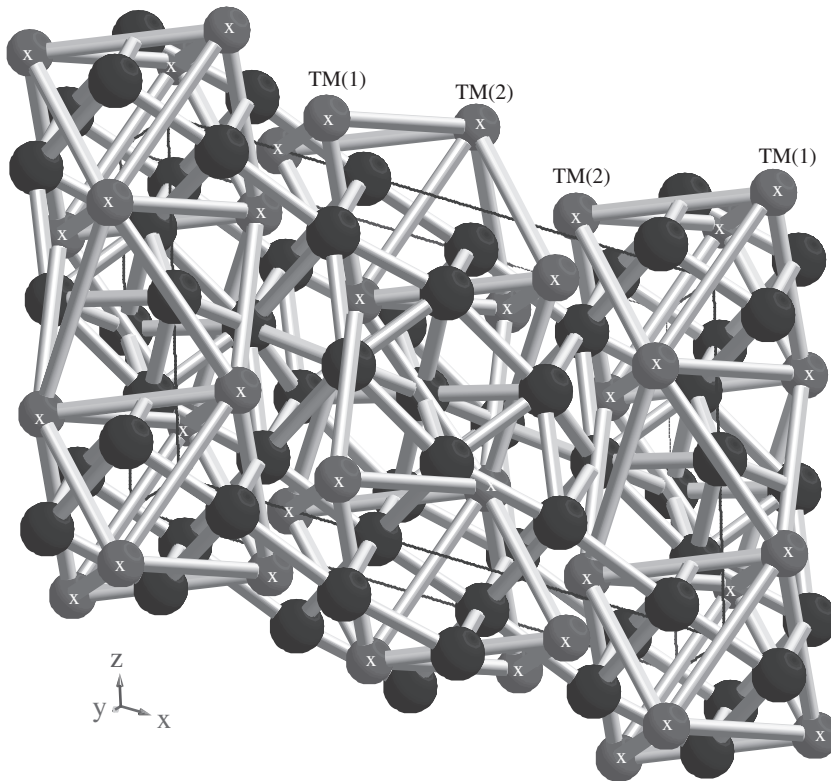


Figure 2. Crystal structure of the X-phase. The dark large spheres are Al atoms, the smaller grey spheres (marked by white x) are TM atoms. The unit cell is marked. The distances between TM atoms at the vertices of the octahedra (marked by stick bonds) are between 4.07 and 4.76 Å, Al-Al distances (marked by stick bonds) range from 2.6 to 3.3 Å.

Relaxed total energies are converted to enthalpy of formation ΔH by subtracting off a composition-weighted average of pure bulk elemental energies [11]. Specific structures and enthalpies may be viewed on the WWW at [12].

We found the experimental structure resulted in small forces (average $0.16 \text{ eV}/\text{\AA}$) indicating the refined atomic positions are accurate. Examination of chemical substitution found that the position TM(2) must be occupied by Co. Placing a Ni on a TM(2) site raises the energy by at least 0.28 eV above our best structure. In contrast, TM(1) can hold either Co or Ni. This has been checked in the low-symmetry (Cm) trial structure and is also fully compatible with spacegroup $C2/m$. The lowest-energy variants have composition $\text{Al}_{18}\text{Co}_5\text{Ni}_3$, with one Co on a TM(1) site and the remaining TM(1) sites all Ni.

The coordination polyhedron ($<3 \text{ \AA}$) around the pure Co site TM(2) consists of 10 Al plus 1 TM(1). That around the mixed position TM(1) is surrounded by 8 Al plus 2 TM(1) plus 1 Co on TM(2). Consequently, the Co atoms are surrounded by a larger number of Al atoms than the TM(1) position, which is in 3 of 4 cases Ni. On the other hand, the TM(1) site has more TM neighbours, which are mainly Ni.

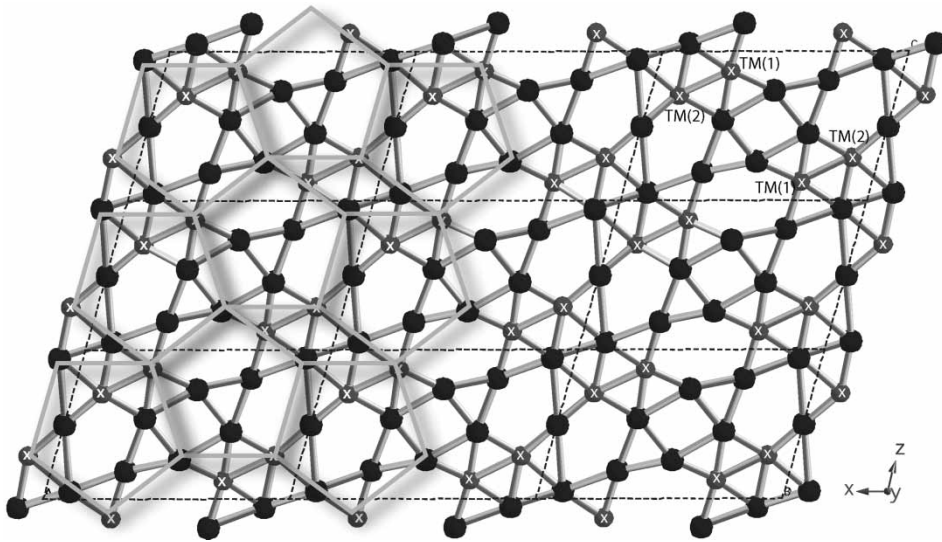


Figure 3. One layer of the X-phase ($y=0$) with pentagonal structure motifs indicated. The other layer is symmetrically equivalent by C centring. 3×3 unit cells are shown (dark large spheres are Al atoms, smaller grey ones, marked by white x, are TM atoms). The pentagonal network is scaled by a factor 1.02 along the a direction to match lattice parameters. The TM(1) position is occupied by Co/Ni, TM(2) by Co.

This agrees with results for other approximants where it is also found that the number of Ni–Ni contacts is greater than Ni–Co or Co–Co, and can be attributed to Co binding to Al more strongly than Ni does [13].

Even our best structures remain energetically unfavourable, with enthalpy of 6 meV/atom greater than a mixture of Al_5Co_2 , Al_3Ni_2 , and either AlCo or Al_3Co , indicating low temperature instability. However, the Co/Ni disorder on TM(1) sites gives a considerable entropic contribution to the free energy, suggesting a mechanism for high temperature stability.

A crude calculation of the entropy neglects correlations among the chemical occupancy of the TM(1) sites. Denoting the mean Co occupancy of each TM(1) site by x , we write the entropy of each TM(1) site as $s = -k_B (x \ln x + (1-x) \ln(1-x))$. Since each 26-atom cell contains 4 TM(1) sites, this configurational entropy reduces the free energy per atom by $\alpha G = (4/26) Ts$. Setting x to the energetically favoured value $x=1/4$ yields $\alpha G = 8.9$ meV/atom at the $T=1200$ K annealing temperature, sufficient to overcome the 6 meV/atom relative enthalpy of the X phase. More careful evaluation of the full partition function (relaxing the constraint on x and including calculated energies) supports this conclusion.

Most specific individual arrangements of Co on TM(1) sites lower the symmetry from $C2/m$ to Cm . However, the full ensemble of configurations maintains the higher symmetry, and hence the structure will exhibit $C2/m$ symmetry unless occupancy correlations develop leading to a global symmetry breaking.

5. Conclusions

The X-phase bears some resemblance to the other approximants of decagonal Al–Co–Ni since it is built from similar pentagonal prismatic basic units. It could even be seen as a kind of Ni-stabilized m -Al₁₁Co₄, with some Al replaced by Ni resulting in half the a lattice parameter and symmetry increased from $P2$ to $C2/m$. It is remarkable that despite of its two-layer periodicity, the X-phase is in equilibrium with the four-layer modification of decagonal Al–Co–Ni and not with the two-layer basic Ni-rich one. Thus, the X-phase could be considered as a continuation of the two-layer decagonal phase at its lowest possible Al concentration towards lower Ni contents. Therefore, in a sample in the two-phase field $D + X$, the four-layer Al-rich decagonal Al–Co–Ni coexists with the two-layer Al-poor approximant (X) of the basic Ni-rich decagonal phase.

The combination of X-ray structure analysis with quantum-mechanical calculations proved to be successful. It confirmed not only the results of the X-ray structure analysis, *i.e.* the stability of the refined structure model, but it also allowed us to get an insight into Co/Ni ordering.

Acknowledgements

W.S and S.K. gratefully acknowledge financial support from grant SNF 200020-105158, M.M. from grant VEGA-2/5096/25 and M.W. from NSF grant DMR-0111198. W.S. would like to thank Yuri Grin for valuable discussions.

References

- [1] S. Kek, PhD thesis, University of Stuttgart, Germany (1991).
- [2] T. Gödecke, M. Scheffer, R. Lück, *et al.*, *Z. Metallkd.* **89** 687 (1998).
- [3] M. Scheffer, T. Gödecke, R. Lück, *et al.*, *Z. Metallkd.* **89** 270 (1998).
- [4] R. Lück, M. Scheffer, T. Gödecke, *et al.*, *Mater. Res. Soc. Symp. Proc.* **553** 25 (1998).
- [5] Available online at: <http://www.oxford-diffraction.com/crysalis.htm>.
- [6] G. Sheldrick, SHELXS-97, *Program for the Solution of Crystal Structures* (University of Göttingen: Germany, 1997).
- [7] G. Sheldrick, SHELXL-97, *Program for the Refinement of Crystal Structures* (University of Göttingen, Germany, 1997).
- [8] W. Steurer, *Z. Kristallogr.* **219** 391 (2004).
- [9] G. Kresse and J. Hafner, *Phys. Rev. B* **47** RC558 (1993).
- [10] G. Kresse and J. Furthmüller, *Phys. Rev.* **54** 11169 (1996).
- [11] M. Mihalkovic and M. Widom, *Phys. Rev. B* **70** 144107 (2004).
- [12] Available online at: <http://alloy.phys.cmu.edu>.
- [13] M. Mihalkovic, *et al.*, *Phys. Rev. B* **65** 104205 (2002).